

MECHANICAL BEHAVIOR OF DOUBLE-SKINNED COMPOSITE STEEL TUBULAR COLUMNS

Min-Lang Lin and Keh-Chyuan Tsai

National Center for Research on Earthquake Engineering, Taipei, Taiwan

mllin@ncree.gov.tw, kctsai@ncree.gov.tw

Abstract

The purpose of this experimental study is to investigate the behavior of the double-skinned concrete filled steel tubular (DSCFT) columns on the strength, stiffness and ductility performance. The diameter-thickness (D/t) ratio and the hollowness ratio were chosen as main parameters in designing the specimens. A total of 18 specimens were tested under varied combinations of axial and flexural loads, and two specimens were tested under a combination of constant axial load and cyclically increasing bending for comparison. Test results concluded that the DSCFT columns can effectively provide strength and deformation capacity even with a large D/t ratio.

INTRODUCTION

Double-skinned concrete filled steel tubular (DSCFT) columns consisting of two concentric circular thin steel tubes with filler between them have been investigated for different applications. It has been used for vessels under external pressure in very deep water (Montague et al. 1975) and for compression member in offshore constructions (Wei et al. 1995). Compare to concrete-filled steel tubular (CFT) columns, the DSCFT can reduce its own weight while have a high flexural stiffness. Compare to traditional RC bridge columns, the DSCFT columns can reduced the requirements on labor and construction time. The construction quality can be easily maintained. Due to these benefits, some researchers have investigated the DSCFT for high rise bridge applications (Hsu et al. 2000, Fumio et al. 2000). The land of Taiwan is mountainous; thus the construction of high rise bridge columns is rather common. Therefore, the DSCFT columns may be a promising choice for the construction of high rise bridge columns.

EXPERIMENTAL PROGRAM

Fabrication of Specimens

Fig. 1 and Table 1 show the typical dimensions of specimens tested in this study. The effective length of the specimens is 1100 mm, and the external and internal diameters are 300 and 180 mm, respectively. A36 steel and 28 Mpa concrete are used for all specimens. The specimens can be separated into 3 series: SS-2, DS-06-4-2 and DS-06-2-2. Series SS-2 is the CFT columns for comparison, where the SS denotes the single skinned tube and the thickness of the tube is 2 mm.

DS-06-4-2 series is the DSCFT columns with a 0.6 hollowness (internal to external diameter) ratio, the thickness of the external and the internal steel tubes are 4 and 2 mm, respectively. The corresponding diameter-thickness ratio (D/t) is 100 and 90 for external and internal tubes, respectively. DS-06-2-2 series is with a 0.6 hollowness ratio, and both the external and internal steel tube thicknesses are 2 mm. The corresponding D/t ratios are 150 and 90 for external and internal, respectively. The last string in the specimen ID denotes the experimental method, where C stand for concentric axial loading, E for eccentric axial loading. For example, SS-2-C means SS-2 series specimen subjected to concentric axial loads. If the last string consists of numbers, it represents the applied axial load ratio (in percentage) during four point bending test. The DS-06-4-2-25C and DS-06-2-2-25C denotes the cyclic four point bending test under a magnitude of 0.25 P_n axial load. P_n is the nominal axial strength of the specimen ($P_n = A_s f_y + A_c f'_c$). All the specimens were fabricated using a cold-formed steel plate for each skin.

Table 1 Dimensions of test specimens

Series	Amount	Exter. dia. : D_e (mm)	Inter. dia. : D_i (mm)	Hollow ratio : D_i / D_e	Thick. of exter. Tube : t_e (mm)	Thick. of inter. tube : t_i (mm)	P_n ($=A_s f_y + A_c f'_c$) (kN)
SS-2	4	300	NA	NA	2	NA	2398
DS-06-4-2	7	300	180	0.6	4	2	1940
DS-06-2-2	7	300	180	0.6	2	2	2355

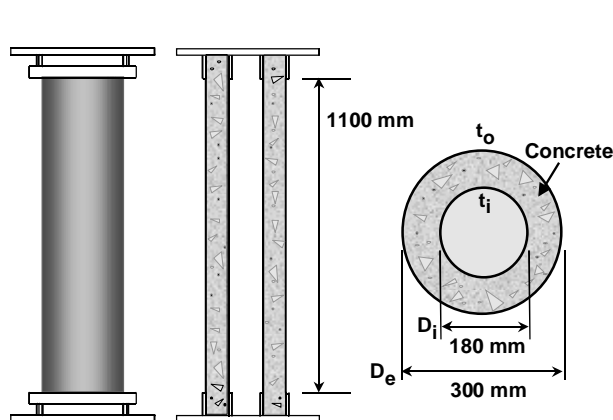


Fig. 1 DSCFT specimen details

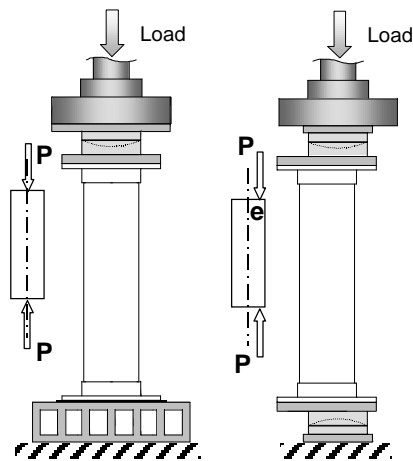


Fig. 2 Setup for axial loading test

Testing Method

Experimental setup for axial loading tests is shown in Fig. 2. The tests were conducted using the Shimadzu 4900 kN universal testing machine with a specified strain rate. Fig. 3 shows the test setup for the four point bending experiment. After the horizontal actuator has applied a specified axial load, then the vertical actuator applied monotonically or cyclically increasing bending to the specimen. The middle region of the beam shown in Fig. 4 is subjected to pure bending. Thus, the specimen can be loaded with a combination of axial load and bending moment.

The THS-1100 data logger and SHW-50D switch box made by TML Company were employed for data collection during the tests. External LVDTs and tiltmeters were used for measuring the deformation and rotation of the specimens. Three-element rosette strain gages were also aligned on tube surfaces of each specimen for further analysis.

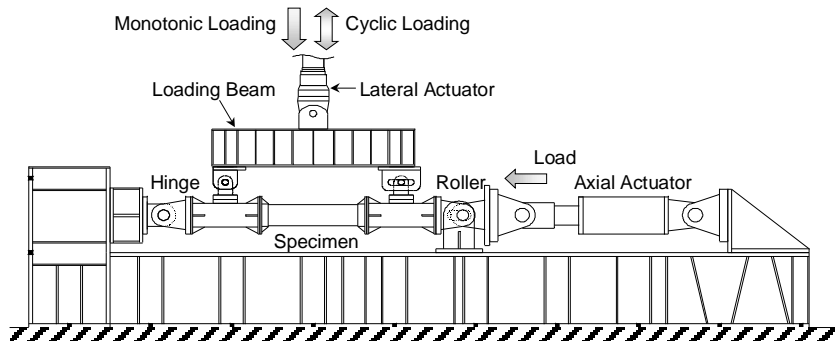


Fig. 3 Setup for four point bending test

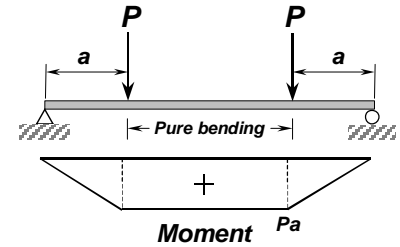


Fig. 4 Four point bending

EXPERIMENTAL RESULTS OF AXIAL LOADING TEST

Experimental results of axial loading test are listed in Table 2. Fig. 5 shows the axial load-strain relationships. The load responses in Fig. 6 are normalized with respect to the corresponding peak axial loads.

Strength Capacity

The strength capacity P_u of a specimen is defined as the peak value of the axial loads observed in the axial load-strain curve. The corresponding strain is denoted as ϵ_p . The value of P_0 is the nominal strength given by Eurocode 4:

$$P_0 = A_s f_{y,t} + A_c f'_c \quad (1)$$

where A_s and A_c are the cross-sectional areas of the steel and concrete section, respectively. The $f_{y,t}$ and f'_c are the yield strength of the steel tube and the actual compressive strength of the concrete. Equation 1 differs from the AIJ specifications where a reduction factor of 0.85 for the core concrete is not considered herein. It is observed that all values of P_u/P_0 are greater than 1.0 but not too significantly. Thus, it appears that Eurocode 4 can conservatively predict the ultimate axial strength of a DSCFT.

Table 2 Results of axial loading test

Specimen	P_u (kN)	P_0 (kN)	P_u/P_0	ϵ_p (%)	E_{comp} (MPa)	E_{the} (MPa)	E_{comp}/E_{the}	μ_{95}
SS-2-C	2846	2464	1.16	0.46	16338	29458	0.55	3.125
DS-06-2-2-C	2311	2081	1.11	0.32	25185	36491	0.69	2.88
DS-06-4-2-C	2750	2567	1.07	0.61	29257	43680	0.66	2.78

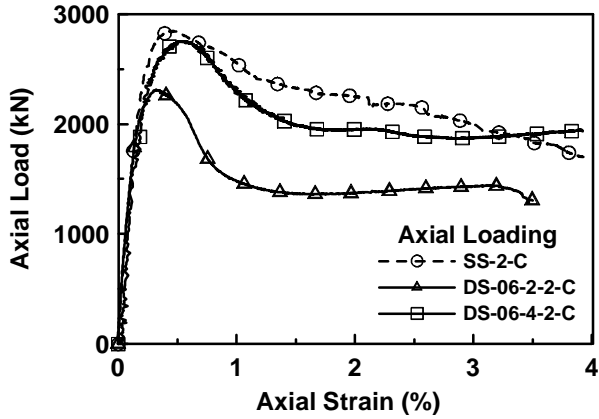


Fig. 5 Axial load-strain curves

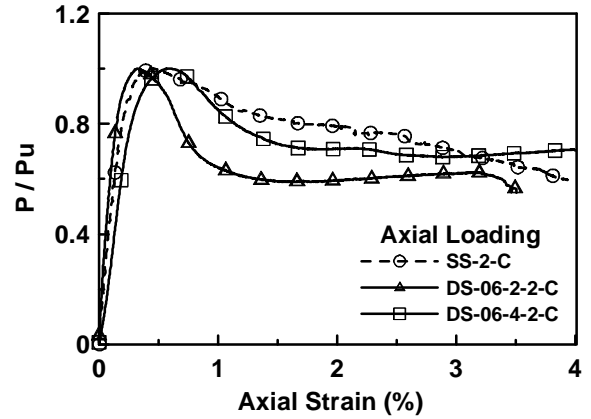


Fig. 6 Normalized load-strain curves

Stiffness

The initial stiffness E_{comp} of a composite member is defined as the averaged initial slope of an axial load-strain curve. It is calculated from its linear recurrence within the range of 0.05% to 0.10% axial deformation, divided by the cross-sectional area A_{total} of the composite member. The theoretical stiffness, according to the theory of superposition can be expressed as:

$$E_{the} = (A_s E_s + A_c E_c) / A_{total} \quad (2)$$

where the modulus of concrete is calculated from $E_c = 4733\sqrt{f'_c}$ Mpa. The values of E_{comp} / E_{the} of all specimens are listed in Table 2. Apparently, the values of E_{the} computed from Equation 2 seriously overestimate the stiffness of the specimen.

Axial Ductility

In this study, the axial ductility is defined as:

$$m_{95} = \frac{e_{95}}{e_y} \quad (3)$$

$$e_y = \frac{e_{75}}{0.75} \quad (4)$$

where e_{75} and e_{95} shown in Fig. 7 are the axial strains corresponding to the 75% and 95% of the peak axial load before and after the peak load was achieved, respectively. Because the yielding point of a specimen is difficult to identify from the axial load versus strain curve, the idealized yield strain e_y is extrapolated from e_{75} .

From Table 2, Figs. 5 and 6, it is observed that all the specimens have similar performance in axial ductility. The ductility value of the CFT specimen is slightly larger than the DSCFT specimens. That is, the strength degrading of the CFT specimen is slightly slower than the DSCFT specimens, but not significantly. When a 0.03 axial strain is reached, all the specimens can still retain more than 50% of

its peak strength.

Table 3 Results of four point bending test

Specimen	Experiment	M_u (kN-m)	EI (10^2 kN-m ²)		$\mu_{90/y}$
			EXP	Theory	
SS-2-0	Four point bending P = 0% P _n	93	129	92	NA
DS-06-4-2-0		182	200	128	NA
DS-06-2-2-0		124	161	95	NA
SS-2-25	Four point bending P = 25% P _n	122	209	92	12.2
DS-06-4-2-25		192	265	128	6.0
DS-06-2-2-25		138	233	95	4.9
DS-06-4-2-40	Four point bending P = 40% P _n	189	230	128	7.1
DS-06-2-2-40		136	221	95	4.0
DS-06-4-2-70	Four point bending P = 70% P _n	122	168	128	3.8
DS-06-2-2-70		107	85	95	1.6

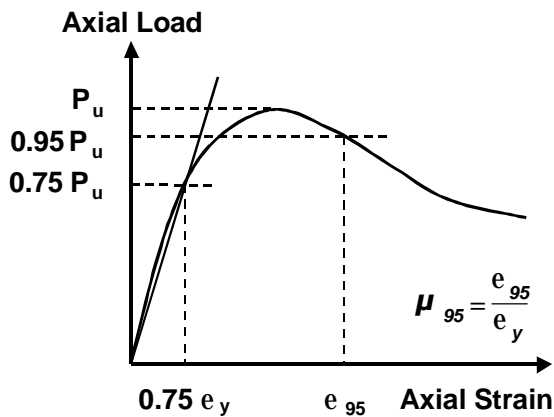


Fig. 7 Axial ductility definition

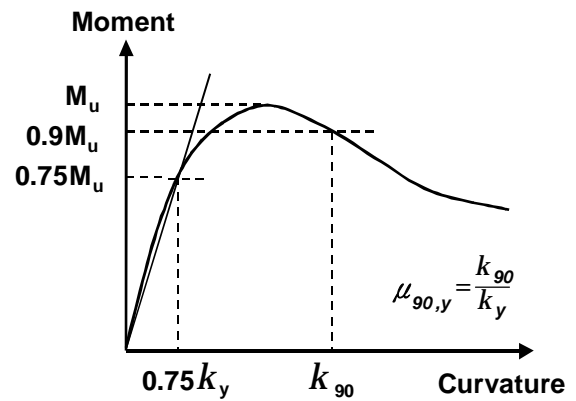


Fig. 8 Curvature ductility definition

EXPERIMENTAL RESULTS OF FOUR POINT BENDING TEST

Moment Capacity

The moment capacity M_u listed in Table 3 is defined as the peak bending in a moment-curvature curve considering the second order effects caused by the horizontal actuator. Comparing with the CFT specimen, the DSCFT specimens developed a larger moment capacity, even in the DS-06-2-2 series

specimens. These specimens have the same external steel thickness (2mm), but it should be noted that DSCFT specimens have a 36% reduction on concrete area and a rather large D/t internal tube.

Flexural Stiffness

The flexural stiffness EI is defined as the averaged initial slope of a moment-curvature curve. And the EI value is calculated from the linear recurrence within the curvature range of $0.05 \times 10^{-2}/m$ to $0.15 \times 10^{-2}/m$. From Table 3, it's observed the variation of the EI have the same trend as the moment capacity of the specimens. The theoretical flexural stiffness (Zhong et. al 1999) adopted here is:

$$EI = (0.6625 + 0.9375 a) (E_s I_s + E_c I_c) \quad (5)$$

where $a = A_s/A_c$, E_s and E_c are the modulus of steel and concrete, I_s and I_c are the moment of inertia of steel and concrete. The experimental EI of the specimens is higher than the theoretical EI . One of the reasons may be due to the constant axial load applied before the bending. The strength and stiffness of the core concrete were enhanced due to the lateral confinement from the steel tube.

Flexural Ductility

In this study, the flexural ductility is defined as:

$$m_{90/y} = \frac{k_{90}}{k_y} \quad (6)$$

$$k_y = \frac{k_{75}}{0.75} \quad (7)$$

where k_{75} and k_{95} (Fig. 8) are the flexural curvatures corresponding to the 75% and 95% of the peak moment before and after the peak load was achieved, respectively. Similar to the axial ductility, the idealized yield curvature k_y is extrapolated from k_{75} .

Table 3 shows the $m_{90/y}$ value of the specimens. It is observed that $m_{90/y}$ value decreases as the axial load ratio increases. The moment-curvature curves for DS-06-2-2 and DS-06-4-2 specimens are shown in Figs. 9 and 10. The degrading speed of the moment capacity is related to the axial load ratio. The normalized moment-curvature curves of the specimens under pure bending and 25% axial load are shown in Figs. 11 and 12. The CFT and DSCFT specimens have very similar performance under these axial load intensities. It should be noted that the degrading of the DSCFT specimen under a 25% axial load is more evident than the CFT due to the buckling of internal tube occurred.

EXPERIMENTAL RESULTS OF CYCLIC FOUR POINT BENDING TEST

The DS-06-4-2-25C and DS-06-2-2-25C were subjected to the cyclic bending loads while an axial load of $0.25P_n$ was maintained. From Figs. 13 and 14, both specimens have the same strength capacity and degrading tendency as those observed in monotonic load tests. The cyclic energy dissipation capacities of these two specimens are rather good as evidenced in their hysteretic responses.

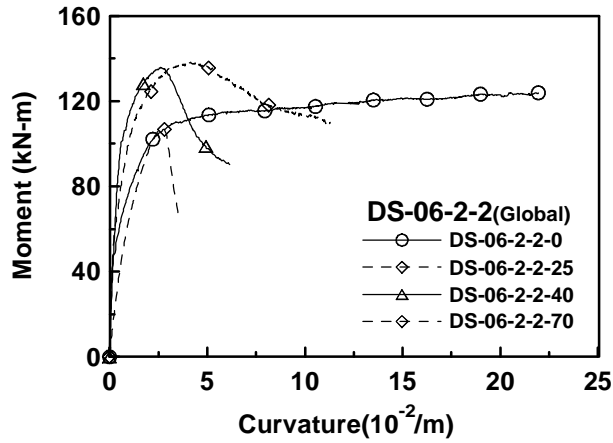


Fig. 9 Moment-curvature response of DS-06-2-2 Series

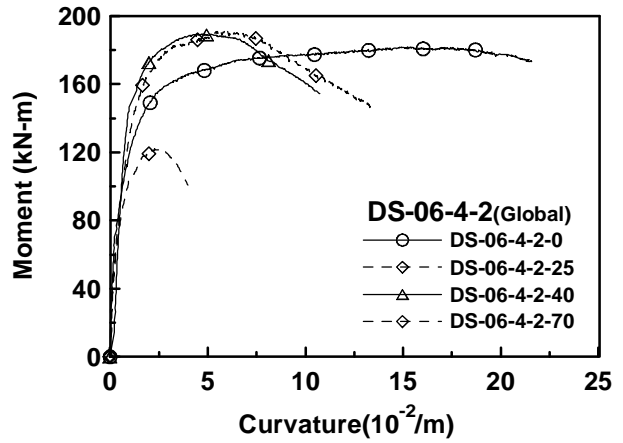


Fig. 10 Moment-curvature response of DS-06-4-2 Series

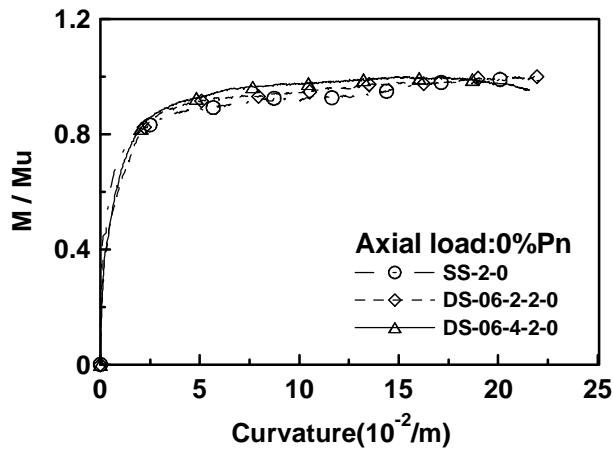


Fig. 11 Normalized moment-curvature curves (0% Pn)

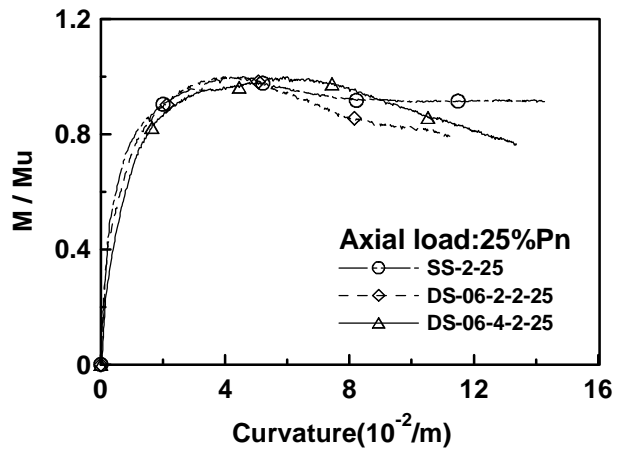


Fig. 12 Normalized moment-curvature curves (25% Pn)

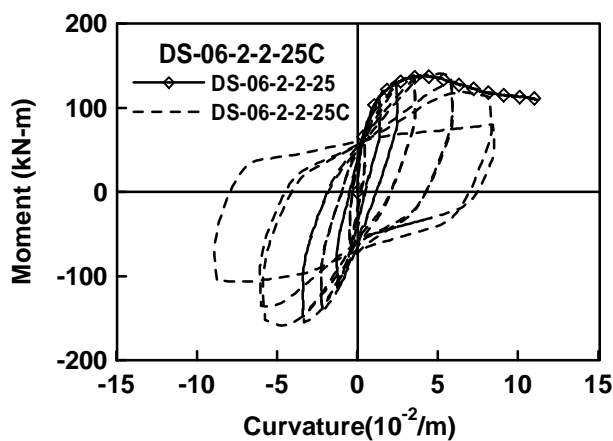


Fig. 13 Moment-curvature response of DS-06-2-2-25 and DS-06-2-2-25C

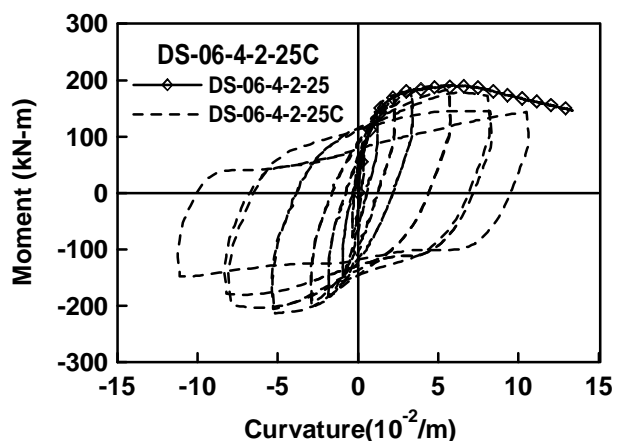


Fig. 14 Moment-curvature response of DS-06-4-2-25 and DS-06-4-2-25C

CONCLUSIONS

1. Superposing the concrete and steel strength can predict the ultimate axial strength of DSCFT conservatively. It is illustrated that steel tube can improve the confinement of the concrete, and the in-filled concrete can delay the occurrence of local buckling of the steel tube with a large D/T ratio.
2. The DSCFT columns can have an optimal strength performance if the applied axial load is less than 40% axial capacity.
3. Experimental results indicate that the behavior of DSCFT columns under cyclic loading is as good as that under the monotonic loading.

REFERENCES

- Montague, P. (1975), "A Simple Composite Construction for Cylindrical Shells Subjected to External Pressure", *J. Mech. Eng. Sci.*, Vol. 17(2), 105-113.
- Wei, S., Mau, S.T., Vupulanadan, C. and Mantrala, S.K. (1995), "Performance of New Sandwich Tube Under Axial Loading: Experiment", *J. Struct. Eng., ASCE*, Vol. 121(12), 1806-1814.
- Fumio Yagishita, Hiroaki Kitoh, Masato Sugimoto, Tsutomu Tanihira, Keiichiro Sonoda (2000), "Double Skin Composite Tubular Columns Subjected to Cyclic Horizontal Force and Constant Axial Force", *Proceedings of 6th ASCCS Conference*, Los Angeles, 497-503.
- Hsu H.L., Lin J.L. (2000), "Inelastic Behavior of Sandwich Box Column under Combined Loading", *Proceedings of 6th U.S. National Conference on Earthquake Engineering*.
- Zhong, S.T. (1999), *Concrete Filled Steel Tubular Structures*.